

Adsorption of the Orange Methyl Dye and Lead (II) by the Cationic Resin Amberlite®IRC-50: Kinetic Study and Modeling of Experimental Data

¹Jaouad Bensalah*, ^{1,2}Mohamed Berradi, ¹Amar Habsaoui, ²Omar Dagdag, ¹Adblhay El Amri, ¹Omar El Khattabi, ¹Ahmed Lebkiti and ¹El Housseine Rifi

¹Laboratory of Advanced Materials and Process Engineering (LAMPE), Department of Chemistry, Faculty of Sciences, Ibn Tofaïl University, B.P. 133, 14000 Kenitra, Morocco.

²Laboratory of Industrial Technologies and Services (LITS), Department of Process Engineering, Height School of Technology, Sidi Mohammed Ben Abdallah University, P.O. Box 2427, 30000, Fez, Morocco. bensalahjaouad11@gmail.com*

(Received on 9th November 2020, accepted in revised form 18th February 2021)

Summary: During this present study, we tested the adsorption performance of heavy metal ions; bivalent lead (Pb (II)) and the anionic dye (methyl orange (MO)) from model aqueous solutions with the ion exchange resin of the Amberlite®IRC-50 type. This performance was evaluated using inductively coupled plasma (ICP) and atomic absorption spectroscopy (AAS). The pH of the solution was adjusted to 6.5 for the bath temperature, the initial mass concentration of Pb (II) and MO was adopted at 20 mg/L, the mass of the resin-type adsorbent Amberlite®IRC-50 was taken at 0.1g and the adsorption capacity Q_e was studied. The results obtained during this study show that the kinetic study of the adsorption was obtained at the contact time $t = 30$ min for the metal Pb (II) and at $t = 60$ min for the dye MO. These results also showed that the equilibrium of adsorption was reached at time $t = 60$ min with an adsorption performance of around 99% for Pb (II) and around 96% for MO. Note that the parameters of different mathematical models indicate that the adsorption process is spontaneous in the second degree.

Key-words: Adsorption, Heavy metals Pb (II), Anionic methyl orange dye, Cationic resin Amberlite®IRC50, Adsorption capacity, Adsorption performance.

Introduction

In the case of a gradual increase in the volume of industrial wastewater discharged directly or indirectly from manufacturing units. This wastewater is generally loaded with biological materials and toxic chemicals, causing an ecological imbalance in aquatic environments [1-3]. Indeed, they have a negative impact on the flora and fauna made up of these aquatic environments [4]. In addition to microorganisms such as bacteria, viruses and fungi, there are also the organic chemicals (oils, fats, dyes, organic pharmaceuticals, etc.), the inorganic (heavy metals) and organometallic (organometallic catalysts, metallocenes, metallocarboranes, carbons, clusters) [5-7]. In addition to their effects on the aquatic environment, they impact, over the medium and long term, on human health after exposure to these chemicals because of their thermal stability and the difficulty of their biodegradability (industrial dyes of textile finishing) under normal ecological conditions [8, 9]. They also have toxicity, mutagenicity and carcinogenicity properties, which makes industrial effluents charged by heavy metals and textile dyes even at very low concentrations much more reducing the penetration of the sun while disturbing the aquatic biological activities of living beings aquatic [10, 11]. In addition to the exploitation of chemicals composed of bivalent lead, Pb (II), methyl orange is

an anionic also dye and is widely used in the laboratory in the textile industry for dyeing textile articles.

According to the requirements indicated by environmental protection laws which involve the elimination and reduction of the content of heavy metals and textile dyes contained in industrial effluents discharged into aquatic environments, there are several techniques and methods of treatment of industrial wastewater such as biological, physical, chemical and physicochemical techniques [12, 13]. In the case of biological techniques, there is aerobic and anaerobic treatment with biological supports, as for the physical treatment there are membrane and incineration processes while that chemical there are techniques of oxidation, reduction, exchange resins ions (REI), coagulation, flocculation and advanced oxidation processes (POA) [14-16]. The adsorption technique is more widely used on a laboratory scale compared to other techniques and processes because of its simplicity, its relatively high efficiency and its ability to remove a wide range of organic and inorganic pollutants [16,17]. Zeolites, clay and activated carbon are among the most effective adsorbents in the adsorption technique due to its large contact surface (300-400m²/g) [18-20]. However,

*To whom all correspondence should be addressed.

their high cost of production and regeneration limits its applicability [21-23]. Whereas artificial cationic resins of the Amberlite[®]IRC-50 type appear to be important for the adsorption of heavy metals (Pb (II)) and the methyl orange dye after studying the adsorption kinetics.


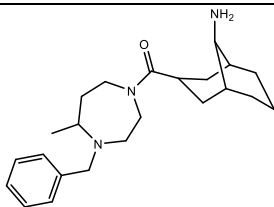

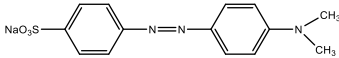

The objective of this study is to decrease the content of Pb²⁺ ions and ions of methyl orange dye (MO) contained in model wastewater synthesized at the laboratory level. While studying the parameters of the adsorption kinetics, such as the initial ion concentration of the Pb²⁺, of the OM, the temperature, the solution pH, the contact time, the stirring speed, the mass of adsorbent, etc. The results obtained are evaluated using AAS, ICP and UV techniques in order to test the possible interactions between the adsorbent and the metal ions Pb²⁺ and the dye MO, on the one hand. On the other hand, they are used in the mathematical modeling of the adsorption process by kinetic models (pseudo first order, pseudo-second order, Elovich, intraparticle diffusion and Bangham).

Experimental

Chemicals used

The chemicals used in this study are the cationic exchange resin Amberlite[®]IRC-50 CAS: 9002-29-3 (Sigma-Aldrich) with the chemical nomenclature 9-Amino-3-bicyclo (3, 3, 1) nonanyl-4-benzyl-methyl-1,4-diazepan-1-yl-methanone and of crude formula C₂₃H₃₇Cl₂N₃O, which is a microporous acrylic polymer used as artificial cationic adsorbents in the form of beads in the synthetic route. Said resin is brought into contact with a solution of hydrochloric acid HCl, at a concentration of 1 M, and then rinsed through several washing cycles with distilled water to purify the adsorbent support and make it neutral. Anhydrate lead nitrate with the chemical formula Pb(NO₃)₂ CAS: 10099-74-8 in the form of a white powder and the anionic dye of the orange or acid orange type 52, in the form of an orange powder, CAS: 547-58-0 of chemical formula C₁₄H₁₄N₃O₃S. The appearance and the chemical formula of these chemicals are grouped respectively in Table 1 below:

Table-1: Appearance and structures of the chemicals exploited.

Chemical products	Aspect	Chemical structure	Molar mass (g/mol)
Amberlite [®] IRC-50			442.5
Orange methyl dye			327.334
Unhydrated lead nitrate		Pb(NO ₃) ₂	331.2

Preparation of model wastewater samples

During this stage, we prepared, on the scale of our laboratory and according to experimental protocols indicated in previous studies [24-26], two model solutions of wastewater loaded separately with the orange methyl dye MO and by lead (II) ions. The first sample was obtained by dissolving 1 g of the MO dye in one liter of distilled water while the second sample was obtained by dissociating a mass of the lead (II) nitrate salt in one liter of distilled water. The stock solutions obtained were used for experimental exploitation in the adsorption technique after a double dilution with distilled water. Note that the new dilutions are prepared and used for each new experiment such that the initial pH of the solutions of the experiment envisaged was adjusted using 0.1 N of nitric acid HNO₃ to have an acid pH and 0.1 N caustic base NaOH to have a basic pH. As the pH of the samples prepared is that which has been adjusted to 6.5 [26].

Calibration curve of prepared model samples

After preparing the model samples, we diluted them by a factor of 10 before any analysis by UV (Ocean Optics spectrometer), at a maximum wavelength of 468 nm, so that the resulting absorbance by relative to the MO concentration is in the linear range. Then, the residual concentration of the MO dye was calculated from the linear calibration curve as a function of the absorbance while using the maximum absorbance peak. While the determination of the concentration of Pb (II) ions was carried out using the atomic absorption spectrometer (AAS) (ICP-AES).

Adsorption of MO dye and Pb²⁺ ions by Amberlite®IRC-50 resin

The content of MO dye and metallic ions of lead (II) was eliminated by the adsorption technique, by adding 0.1 g of Amberlite®IRC-50 resin as adsorbent in a flask containing a volume of 100 ml of sample of prepared model wastewater whose pH is adjusted to the value of 6.5. The mixture obtained was stirred intermittently for an adequate duration and under experimental conditions. As the room temperature is room (25 °C), the concentration of the prepared samples is around 20 ppm and the contact time is calculated at 4 h. After this adsorption period, the obtained water samples were analyzed using atomic absorption spectroscopy (AAS) and ICP to

detect the content of metal ions Pb (II) and by UV spectroscopy to calculate the rest of the MO dye concentration. Note that all these analyze were carried out at the Center for Analysis, Expertise, Transfer of Technique and Incubation at the Faculty of Sciences of Ibn Tofail University, Kenitra-Morocco.

During this adsorption technique of the chemical compounds MO and Pb(II), we calculated respectively the equilibrium (q_e) and instantaneous (q_t) adsorption capacities of the Amberlite®IRC-50 resin based on the equations (1) and (2) and the adsorption yield (R%) by the relation (3) as follows:

$$Q_e = (C_0 - C_e) \times \frac{V}{m} \quad (1)$$

$$Q_t = (C_0 - C_t) \times \frac{V}{m} \quad (2)$$

$$R(\%) = \frac{(C_0 - C_e)}{C_0} \times 100 \quad (3)$$

Knowing that C_0 , C_e and C_t represent, respectively, the initial (steady state) and instantaneous concentrations (ppm) of the analysis that we have carried out, V is the volume (L) of the analytical solution and I am the mass (g) of the Amberlite®IRC-50 resin as an adsorbent.

Results and Discussion

Characterization of Amberlite®IRC-50 before and after adsorption

Washing with HCl and after was loaded with MO dye and metal Pb²⁺ respectively (Fig. 1a, 2b) are shown in are Fig 1. The micrographs of Amberlite®IRC-50 (Fig. 2a, 2b) presenting the presence of microcavities on the surface of the cationic resin raw Amberlite®IRC-50, which indicate a porous and irregular structure that is favorable for adsorbents. However, (Fig. 2b) shows intense white clouds formed due to MO dye and Pb²⁺ adsorption.

The support washed with acid in order to removal the traces of copper. The obtained spectrum after adsorption of MO and Pb²⁺ on the Amberlite®IRC-50 (Fig 3) shows The EDX diagram a significant peak corresponding to the chlorine from the dye following the complexation reaction

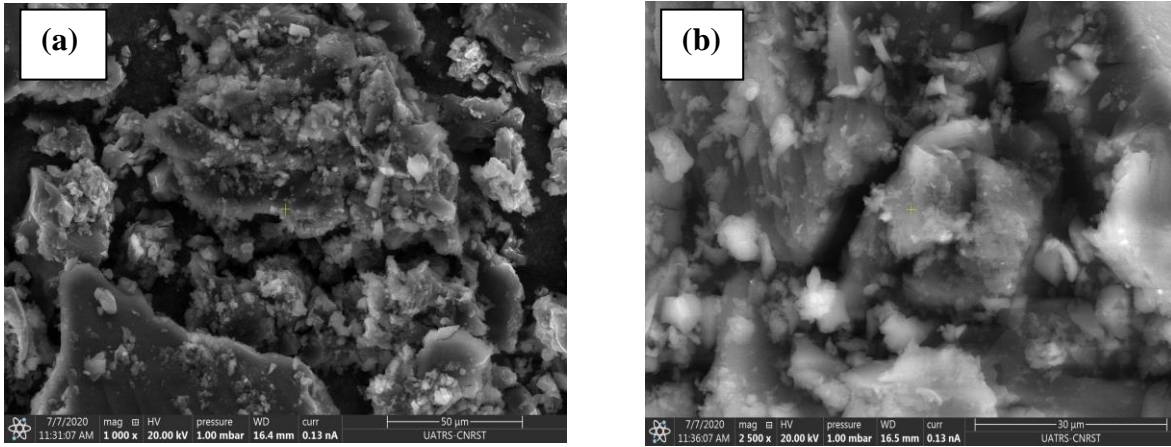


Fig. 1: SEM observation of Amberlite[®]IRC-50 without treatment (a) after being loaded with MO and (b) after being loaded with Pb²⁺.

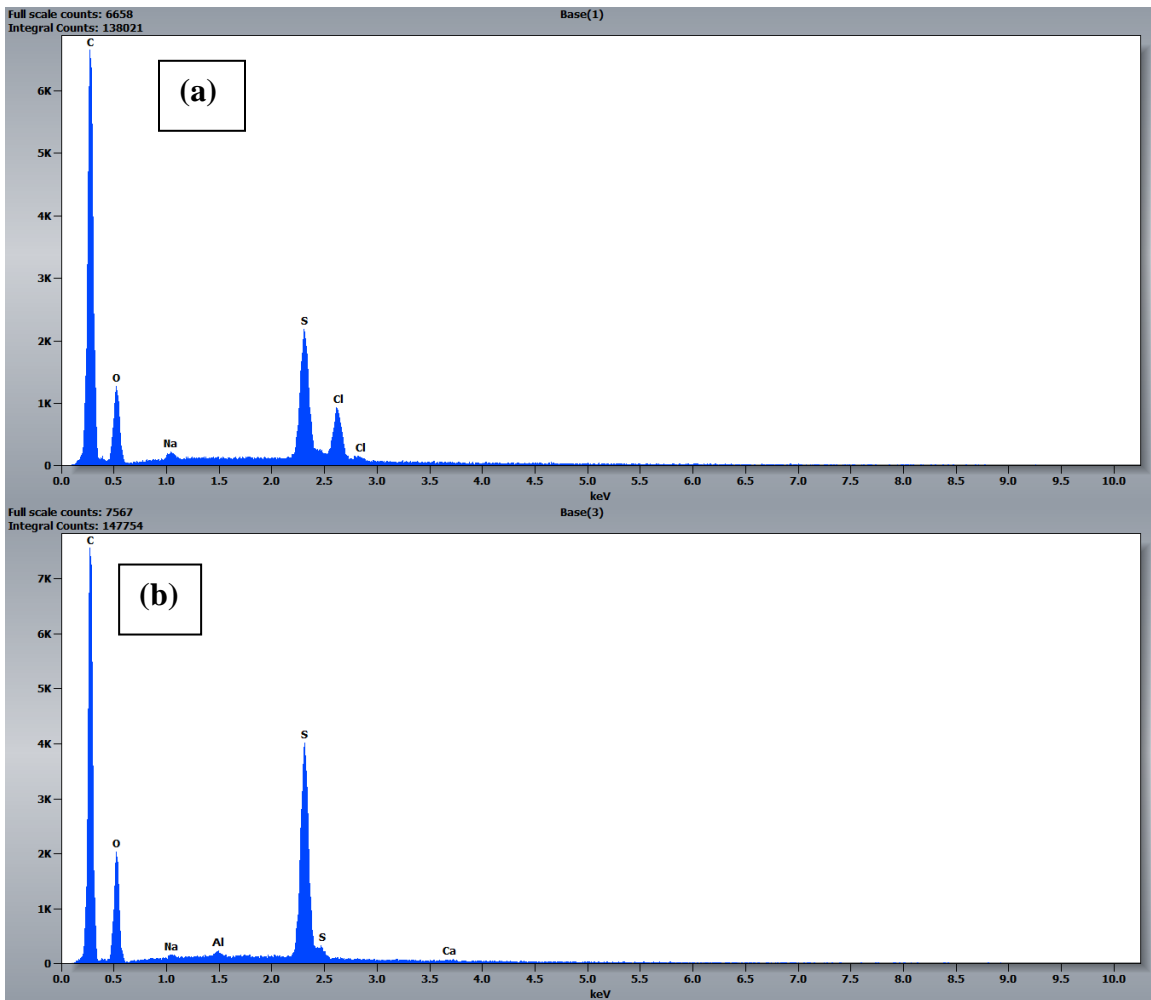


Fig. 2: EDX analysis of Amberlite[®]IRC-50 powder (a) after MO adsorption and (b) after Pb²⁺ adsorption.

Kinetic study of adsorption

In order to find the time necessary to reach the equilibrium of the adsorption of the anionic dye (MO) and the ionic metal Pb (II) by the cationic resin Amberlite®IRC-50, we carried out a kinetic curve up to 120 min as it is shown in Fig. 3.

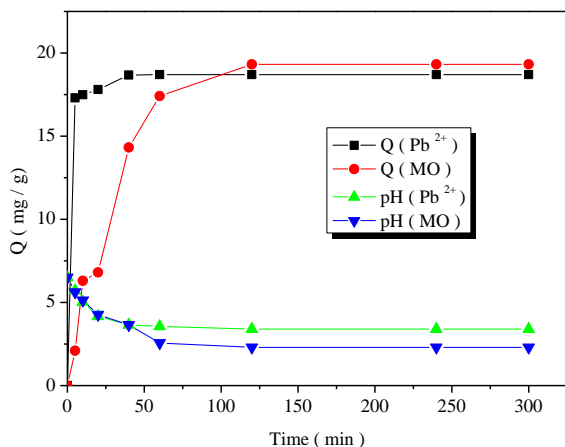


Fig. 3: Kinetics of adsorption of MO and Pb (II) by Amberlite®IRC50 resin as a function of contact time.

From the curves of Fig 1, we see that the adsorption capacity was better at 30 min for the metal Pb(II) and at 60 min for the cationic dye MO. At about 60 min, it was also noticed a first step which is fast followed by a small amount of posterior adsorption. According to this kinetic study, the sites of adsorption by Amberlite®IRC-50 resin were gradually occupied by ions of the MO dye and the metal Pb²⁺.

According to the curves in Fig 1, the maximum adsorption capacity was about 19.50 mg/g for the MO dye and about 18.70 mg/g for the metal Pb(II) which follows a simultaneous evolution pH value, contact time and adsorption capacity Q_e . This increase in the adsorption capacity with respect to these micropollutants is accompanied by a drop in the pH values which decreases from 6.5 to 2.3 for OM and to 3.4 for Pb(II). The results obtained are quite similar to those already obtained in previous studies with the dye MO on the hausmanite magnetic nanoparticle[27].

Kinetic adsorption models

In this present study, the adsorption kinetics were evaluated using kinetic models such as pseudo-

first order and pseudo-second order to determine the mechanisms of adsorption of the micropollutants used.

Pseudo-first order kinetic model

The pseudo-first order kinetic model is expressed according to the following equation (4):

$$\frac{dq_t}{dt} = K(q_e - q_t) \tag{4}$$

Where q_t (mg/g) is the adsorption quantity of micropollutants MO and Pb (II) at each instant t , q_e (mg/g) is the adsorption capacity at equilibrium and K_1 (min⁻¹) is the pseudo-first order velocity constant.

Under the initial conditions $q_t = 0$ at $t = 0$ and by integrating equation (4), we obtained equation (5) which is expressed as follows:

$$\log(q_e - q_t) = \log(q_e) - \left(\frac{k_1}{2.203}\right)t \tag{5}$$

Knowing that K_1 and we were calculated from the slopes and extrapolations of logarithmic plots ($q_e - q_t$) with respect to time to which are listed in Table 2 below. The variation of the pseudo-first order is given according to the following Fig 4:

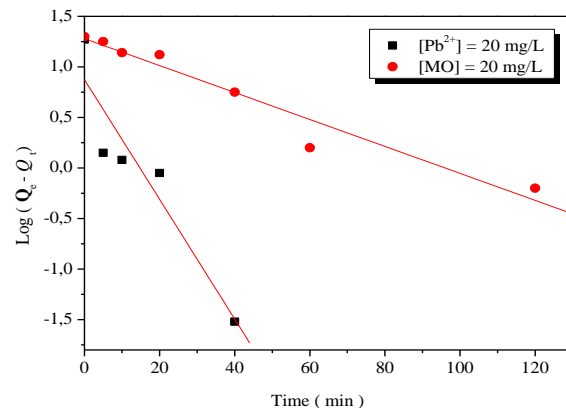


Fig. 4: Pseudo-first order kinetic model of the adsorption of MO and Pb (II) by the Amberlite®IRC-50 resin.

Pseudo-second order model

The pseudo-second order kinetic model is expressed in the form of the following equation (6):

$$\frac{t}{q_t} = \frac{1}{k_2 q_e^2} + \frac{1}{q_e} \times t \tag{6}$$

Where k_2 is the pseudo-second order constant (g/mol.min) and q_e (mg/g) is the adsorption capacity at equilibrium. The lines in Fig 5 below represent the variation of the equation (6) as a function of time.

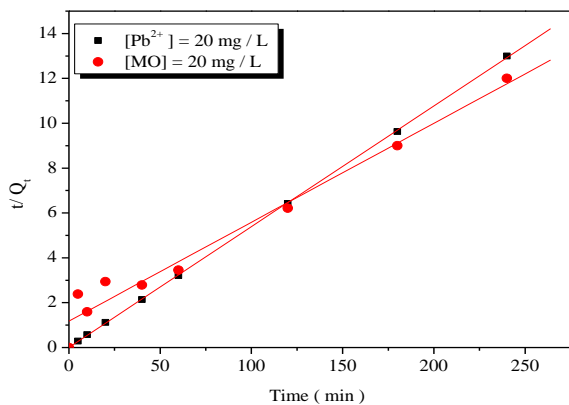


Fig. 5: Pseudo-second order kinetic model of the adsorption of MO and Pb (II) by the Amberlite®IRC-50 resin.

The values of q_e and k_2 can be obtained from the slope and the intersections of the t/q_t curves with respect to the data grouped in Table 2 below.

From Table-2, it turns out that the value of the correlation R^2 of the lines for a better fit using the pseudo-second order of the kinetic equation (6) is of the order of 0.9999. The theoretical equilibrium calculated for the adsorption capacity (q_{e-cal}) is of the order of 18.86 mg/g for the metal ions Pb^{2+} and the experimental adsorption capacity (q_{e-exp}) obtained is of the order of 18.70 mg/g. This indicates that the theoretically calculated values are very close to those which are obtained experimentally. Indeed, according to these results obtained, it turns out that the pseudo-second order kinetic model is verified which allowed us to conclude that the nature of the adsorption exploited of the Pb^{2+} ions by the Amberlite®IRC-50 resin is undergone by physisorption[28].

Table-2: Parameters of the pseudo first order and pseudo second order kinetic model of MO and Pb (II).

Pseudo-first order	$q_{e-exp}(mg/g)$	$q_{e-cal}(mg/g)$	$K_1(min^{-1})$	R^2
[Pb^{2+}]	18.70	7.50	0.1358	0.94
[MO]	20	19.50	0.029	0.992
Pseudo-second order	$q_{e-exp}(mg/g)$	$q_{e-cal}(mg/g)$	$K_2(min^{-1})$	R^2
[Pb^{2+}]	18.70	18.86	0.1326	0.999
[MO]	20	22.72	0.00164	0.996

Elovich's model

To describe the adsorption capacity, which decreases exponentially with an increase in the amount of adsorbent, a kinetic chemisorption equation (7) has used whose following expression:

$$\frac{dq_t}{q_t} = \alpha e^{(\beta q_t)} \tag{7}$$

With α is the initial adsorption constant (mg/g.min) and β is the desorption constant (g/mg) linked to the activation energy for chemisorption. In order to simplify this equation [29], an integration was made under the initial conditions ($t = 0, q_t = 0$ and $t = t, q_t = q_t$), which made it possible to give the following equation (8):

$$q_t = \frac{1}{\beta} \times \ln(\alpha\beta) + \frac{1}{\beta} \ln(t) \tag{8}$$

This equation (8) is used to correlate the experimental data by plotting the curves $q_t = f(\ln(t))$ which are represented in Fig 6 below, such that the constants α, β and R^2 are grouped in Table 3 below.

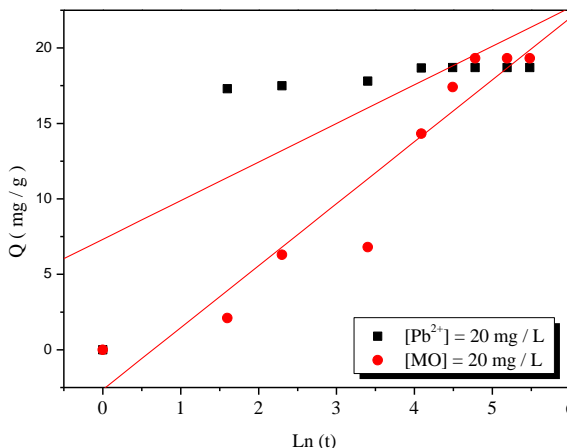


Fig. 6: Elovich kinetic model for the adsorption of MO and Pb (II) by the Amberlite®IRC-50 resin.

Table-3: Kinetic parameters of Elovich model.

Amberlite®IRC-50	α (mg/g.min)	β (g/mg)	R^2
[Pb ²⁺]	2.52	0.24	0.96
[MO]	44.54	0.39	0.77

From Table 3, it turns out that the value of R^2 for the Pb²⁺ ions is quite far from unity ($R^2 > 0.75$). This shows that the amount of adsorption of these ions by the Amberlite®IRC-50 resin is significant compared to that of the MO dye. While the β desorption constant of Pb (II) for Amberlite®IRC-50 resin is lower than that of MO dye.

Intraparticle diffusion model

The intraparticle diffusion model (Weber and Morris model) [30], is used to highlight the type of diffusion mechanism that occurs during the adsorption phenomenon [31]. It is expressed according to the following equation (9):

$$q(t) = K_i \times t^{1/2} + X_i \tag{9}$$

Where K_i is the intraparticle diffusion constant (mol/g.min^{1/2}) and X_i is the value of the thickness of the boundary layer.

The modeling of the experimental results according to the intraparticle model can present a multi-linearity which corresponds to the existence of two successive stages of the adsorption phenomenon. The first step corresponds to a limitation of the adsorption by external diffusion while the second step corresponds to a state of equilibrium where there is no longer any change in the adsorption capacity. The correlation coefficients R^2 is less than 0.975 for the adsorption of two micropollutants. Indeed, the straight lines obtained do not pass through the origin of the reference mark in each case as indicated in Fig 7. Moreover, if only intraparticle diffusion is involved in the process, the line $q_t = f(t_{1/2})$ passes through the origin [32].

Table-4 below groups together the various intraparticle diffusion parameters which are extracted from the curves in Fig 5.

Table-4 : Intraparticle diffusion parameters.

Resin	Concentration (mg.l ⁻¹)	Time (min)	K_i	X_i	R^2
Amberlite®IRC-50	[MO]	<60	1.866	-0.913	0.975
		>60	0.157	17.684	0.894
	[Pb ²⁺]	<60	1.454	8.183	0.702
		>60	0.022	18.45	0.833

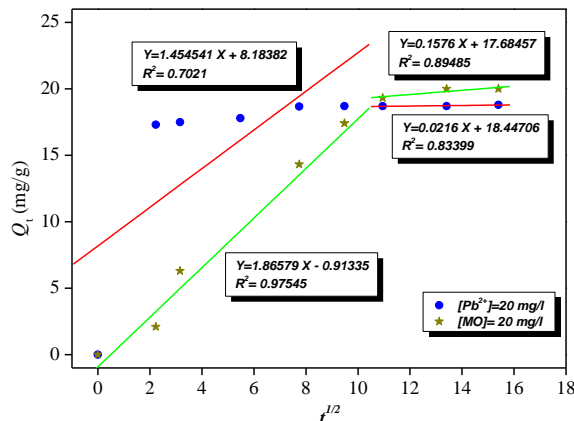


Fig. 7: Modeling of the adsorption kinetics by the intraparticle diffusion model.

Bangham's Model

Bangham's kinetic model explores the slow pore diffusion stage of the adsorption process which is well defined by equation (10)[33]:

$$\text{Log} \left(\text{Log} \left(\frac{C_0}{C_0 - q_{t,m}} \right) \right) = \text{Log} \left(\frac{K_2}{2.303 \times V} \right) + \alpha \text{Log}(t) \tag{10}$$

C_0 is the initial concentration of adsorbate (mg/L), V is the volume of the solution (mL), m is the mass of adsorbent (g), q_t is the quantity (mg/g) of micropollutants adsorbed at time t , α and K_B are constants. In this model, when the curve $\text{Log}(C_0/C_0 - (q_t.m)) = f(\text{log}(t))$ is linear, the adsorption is controlled by the phenomenon of diffusion in the pores. The results are shown in Fig 8 and the kinetic parameters are collated in Table 5.

The linearity of the curves obtained and the values of the correlation coefficients indicated in Fig 6 shows that for the metal of Pb (II) exceeds 0.9, on the other hand, that for the dye MO does not exceed 0.9. This allowed to say that the Amberlite®IRC-50 resin is not compatible with the Bangham model.

Table 5: Kinetic parameters of the Bangham model.

Amberlite®IRC-50	α	K_B	R^2
[Pb ²⁺]	0.025	0.009	0.91
[MO]	0.444	0.0012	0.87

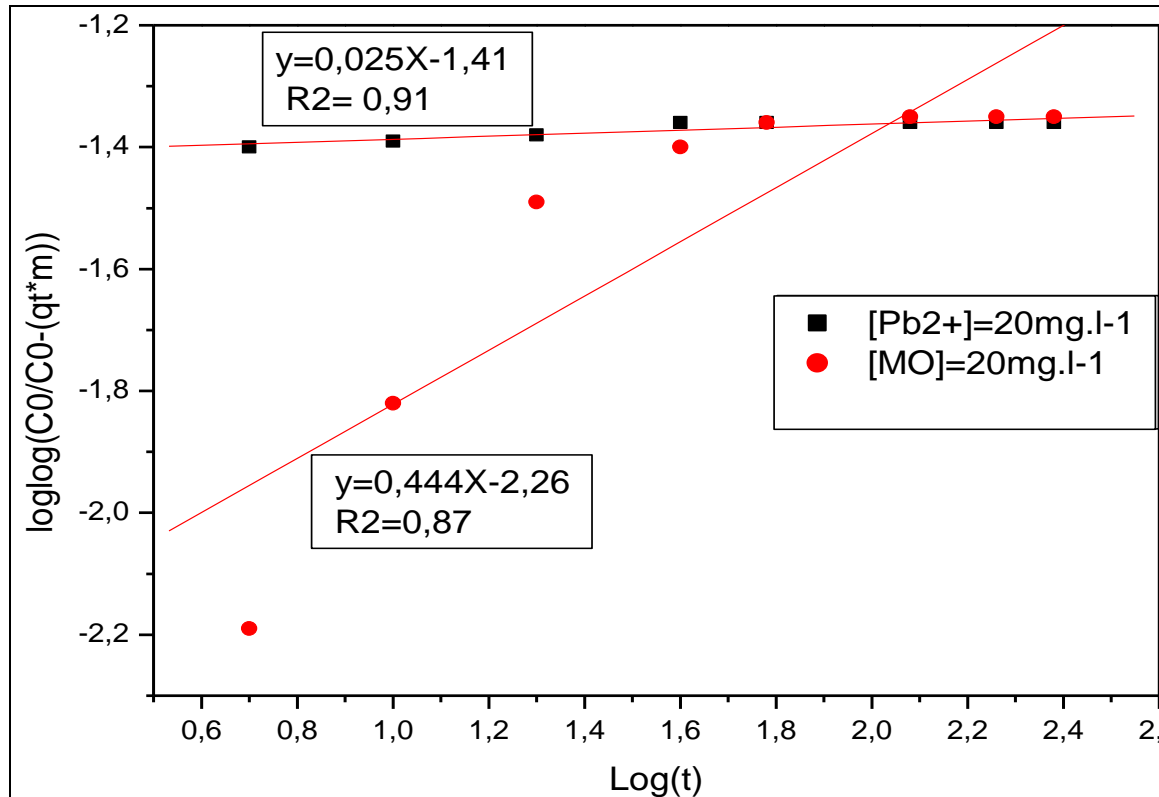
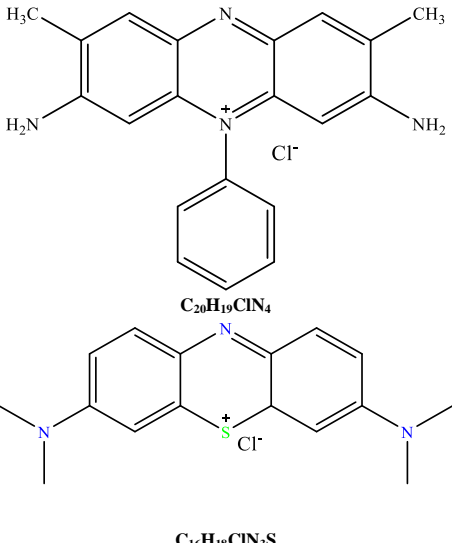


Fig. 8: Modeling of the adsorption kinetics according to the Bangham model ($C_0 = 20 \text{ mg/L}$).

Table-6: Comparative study with our work.

type	Chemical structure and formula	Support	result	References
<p>Safranin-T (SF)</p> <p>AND</p> <p>Methyl orange (MO)</p>	<p>$C_{20}H_{19}ClN_4$</p> <p>$C_{14}H_{14}N_3NaO_3S$</p>	<p>Studies on elimination of the cationic safranin-t and the anionic methyl orange dyes from aqueous solution utilization NaX zeolite synthesized from FLY ASH</p>	<p>Elimination of dyes over the regenerated zeolites is only 68% whereas %elimination of the anionic dye MO over the fresh zeolite is 78%.</p> <p>The adsorption equilibrium is reached after 10h of two dyes. ΔH (-20.18kj.mol⁻¹). ΔS°(-90.32j.mol⁻¹).</p>	[34]

<p>Safranin (SF) And Methylene blue (MB)</p>	 <p>$C_{20}H_{19}ClN_4$</p> <p>$C_{16}H_{18}ClN_3S$</p>	<p>Photocatalytic degradation of the cationic dyes methylene blue and safranin utilization chitosan zinc oxide nano-beads with <i>Musa paradisiaca</i> L. pseudo stem.</p>	<ul style="list-style-type: none"> The efficiency of the photocatalytic degradation was identified as 96.15 and 95.65 % (at 10 hrs) with free zinc nanoparticles, and 97.47 and 96.35 % (at 1.0 hr) for chitosan immobilized zinc oxide nano-beads for the methylene blue and safranin (10.0 ppm) dyes. 	[35]
Lead (II)	<p>$Pb(NO_3)_2$</p>	<p>Adsorption of Heavy metal lead (II) ions from water solutions with natural zeolite and chamotte clay</p>	<ul style="list-style-type: none"> The maximum uptake of lead ions (q_{max}) was determined as 14 mg/g for zeolite and 11 mg/g for clay. 	[36]

Conclusion

In the light of this present study, we can conclude that the adsorption of micropollutants MO and Pb (II) contained in model effluents by the artificial resin Amberlite®IRC-50 was exploited to reduce their content compared to the starting samples.

The equilibrium of the adsorption was as contact time obtained after 60 min of MO dye and 30 min of leads Pb (II) with a low mass of using cationic resin Amberlite®IRC-50 as 0.1 g, and at pH value of 6.5.

The adsorption capacity of the anionic dye MO and of the leads Pb (II) by the cationic resin respectively 20 mg/g and 18.70 mg/g .

The kinetic study of the adsorption technique studied was modeled by different kinetic models such as that of pseudo-first order kinetic model, Pseudo-second order-model, Elovich's model, Intraparticle diffusion-model and Bangham's Model.

These models of the adsorption technique used are well justified by the pseudo-second order model with respect to the metal ions Pb^{2+} . The mechanisms of adsorption are more complex and probably have a combination of mass transfer and intraparticle diffusion. The application of the

technique of adsorption of micropollutants leads Pb (II) and methyl Orange MO by the cationic resin Amberlite®IRC-50 has proven their effectiveness in the treatment of wastewater.

References

- H. Es-sabbany, M. Berradi, S. Nkhili, R. Hsissou, M. Allaoui, M. Loutfi, Removal of heavy metals (nickel) contained in wastewater-models by the adsorption technique on natural clay, *Materials Today: Proceedings*, **13**, 866 (2019).
- J. El Addouli, A. Chahlaoui, A. Berrahou, A. Chafi, A. Ennabili, and L. Karrouch, Influence des eaux usées, utilisées en irrigation, sur la qualité des eaux de l'Oued Bouishak-région de Meknes (centre-sud du Maroc), *Rev. Microbiol. Ind. San et Environn.*, **3**, 56 (2009).
- B. Seyhi, P. Droguil, G. Buelna, J.-F. Blais, and M. Heran, Current state of knowledge of membrane bioreactor processes for the treatment and reuse of industrial and urban wastewater, *Rev. Des Sci. De L'Eau.*, **24**, 283 (2011).
- M. Berradi, R. Hsissou, M. Khudhair, M. Assouag, O. Cherkaoui and A. El Bachiri, Textile finishing dyes and their impact on aquatic environs, *Heliyon.*, **5**, pe02711 (2019).
- M. Allaoui, M. Berradi, and A. Elharfi, Synthesis of a new asymmetric semi permeable membrane and based alloy of two polymers PVC

- and PSU. Application in the treatment of a colored solution, *Mor. J. Chem.*, **4**, 251 (2016).
6. C. Feng, L. Chen, Z. Yan & Z. Du, Self-Assembling Behaviour of Polyglyceryl-Modified Silicone Surfactant in Aqueous Solution, *J. Disper sci technol*, **37**, 1532 (2015).
 7. M. Allaoui, M. Berradi, H. Taouil, H. Es-sahbany, L. Kadiri, A. Ouass, J.Bensalah and Said.Ibn Ahmed, Adsorption of Heavy Métaux (nickel) by the Shell Powder of the Coast of Mehdia-Kenitra (Morocco), *Anal.Bioanal. Electrochem.*, **11**, 1547 (2019).
 8. S. Gita, A. Hussan, and T. Choudhury, Impact of textile dyes waste on aquatic environments and its treatment, *Environ. Ecol.*, **35**, 2349 (2017).
 9. M. Berradi, A. Essamri, and A. El Harfi, Discoloration of water loaded with vat dyes by the membrane process of ultrafiltration, *J. Mater. Environ. Sci.*, **7**, 1098 (2016).
 10. M. Berradi and A. El Harfi, Purification of the textile finishing effluents by the ultrafiltration technique, *Int. J. Adv. Chem.*, **2**, 62 (2014).
 11. B. Al-Rashdi, D. Johnson, and N. Hilal, Removal of heavy metal ions by nanofiltration, *Desalination*, **315**, 2 (2013).
 12. M. Berradi and A. El Harfi, Discoloration of charged models wastewater with reactive and dispersed dyes by the combined process of coagulation-ultrafiltration, *J. Mater. Environ. Sci.*, **8**, 1762 (2017).
 13. F. M. Pang, P. Kumar, T. T. Teng, A. M. Omar, and K. L. Wasewar, Removal of lead, zinc and iron by coagulation–flocculation, *J Taiwan Inst Chem Eng.*, **42**, 809 (2011).
 14. A. Paz, J. Carballo, M. J. Pérez, and J. M. Domínguez, Biological treatment of model dyes and textile wastewaters, *Chemosphere.*, **181**, 168 (2017).
 15. M. Berradi, Performance hybridized process of coagulation-ultrafiltration in discoloration of water charged by the textile finishing dyes, *Mor. J. Chem.*, **4**, 33 (2016).
 16. M. Berradi, O. Cherkaoui, and A. El Harfi, Comparative study of the performance on asymmetric membranes ultrafiltration, Application to the bleaching of colored water with vat dyes, *Appl. J. Environ. Eng. Sci.*, **3**, 114 (2017).
 17. A. Bożęcka, M. Orlof-Naturalna, and S. Sanak-Rydlewska, Removal of lead, cadmium and copper ions from aqueous solutions by using ion exchange resin C 160, *Gospod Surowcami Min.*, **32**, 129 (2016).
 18. M. Berradi, O. Berradi, M. Chellouli, R. Hsissou, M. El Bouchti, M. El Gouri, Optimization of the synthesis of ultrafiltration asymmetric membranes based on organic polymers, *Results in Engineering.*, **6**, 100 (2020).
 19. D. Huang, Bo Li, J.Ou, W. Xue, J. Li, Z. Li, T. Li, S. Chen, R. Deng, X. Guo, Megamerger of biosorbents and catalytic technologies for the removal of heavy metals from wastewater, Preparation, final disposal, mechanism and influencing factors, *J. Environ. Manage.*, **261**, 109879 (2020).
 20. M. Balela, N. Intila, and S. Salvanera, Adsorptive Removal of Lead Ions in Aqueous Solution by Kapok-Polyacrylonitrile Nanocomposites, *Materials Today: Proceedings*, **17**, 672 (2019).
 21. A. R. Agcaoili, M. U. Herrera, C. M. Futralan, and M. D. L. Balela, Fabrication of polyacrylonitrile-coated kapok hollow microtubes for adsorption of methyl orange and Cu (II) ions in aqueous solution, *J. Taiwan Inst Chem Eng.*, **78**, 359 (2017).
 22. D. W. O’Connell, C. Birkinshaw, and T. F. O’Dwyer, Heavy metal adsorbents prepared from the modification of cellulose: Review, *Bioresour. Technol.*, **99**, 6709 (2008).
 23. Y. Guo and E. Du, The effects of thermal regeneration conditions and inorganic compounds on the characteristics of activated carbon used in power plant, *Energy Procedia.*, **17**, 444 (2012).
 24. J. Bensalah, A. Habsaoui, B. Abbou, L. Kadiri, I. Lebkiri, Adsorption of the anionic dye methyl orange on used artificial zeolites: kinetic study and modeling of experimental data, *Mediterr. J. Chem.*, **9**, 311 (2019).
 25. F. Z. Mahjoubi, A. Khalidi, A. Elhalil, and N. Barka, Characteristics and mechanisms of methyl orange sorption onto Zn/Al layered double hydroxide intercalated by dodecyl sulfate anion, *S. Afr. j. sci.*, **6**, e00216 (2019).
 26. Y. Essaadaoui, A. Lebkiri, E. Rifi, L. Kadiri, and A. Ouass, Adsorption of lead by modified Eucalyptus camaldulensis barks: equilibrium, kinetic and thermodynamic studies, *Desalination Water Treat.*, **111**, 267 (2018).
 27. K.L.Bhowmik, A. Debnath, R.K.Nath, S. Das, K.KChahopadhyay, B. Saher, Synthesis and characterisation of mixed phase manganese ferrite and hausmannite magnetic nanoparticle as potential adsorbent for methyl orange from aqueous media artificial neural network modeling, *J. Mol. Liq.*, **219**, 1010 (2016).
 28. V. Arabahmadi & M. Ghorbani, Pb (II) Removal from Water Using Surface Modified Polythiophene-Coated Rice Husk Ash Nanocomposite, *Inorg. Nano-Met. Chem.*, **47**, 1614 (2017).

29. S. Chien and W. Clayton, Application of Elovich equation to the kinetics of phosphate release and sorption in soils, *Can. J. Soil Sci.*, **44**, 265 (1980).
30. W. J. Weber and J. C. Morris, Kinetics of adsorption on carbon from solution, *J Sanit Eng Div Asce.*, **89**, 31 (1963).
31. N. Oladoja, C. Aboluwoye, and Y. Oladimeji, Kinetics and isotherm studies on methylene blue adsorption onto ground palm kernel coat, *Turkish J. Earth Sci.*, **32**, 303 (2009).
32. H. Kaur and R. Kaur, Removal of Rhodamine-B dye from aqueous solution onto pigeon dropping: adsorption, kinetic, equilibrium and thermodynamic studies, *J. Mater Environ Sci.*, **5**, 1830 (2013).
33. I. D. Mall, V. C. Srivastava, N. K. Agarwal, and I. M. Mishra, Removal of congo red from aqueous solution by bagasse fly ash and activated carbon: kinetic study and equilibrium isotherm analyses, *Chemosphere.*, **61**, 492 (2005).
34. Shakti Das and Sanghamitra Barman, Studies on removal of safranin-t and methyl orange dyes from aqueous solution using NaX zeolite synthesized from FLY ASH, *Int. J. Sci., Env. & Tech.*, **2**, 735 (2013).
35. S. Roshitha, V. Mithra, V. Saravannan, S. Senthil Kumar, M. Gnanadesigan: Photocatalytic degradation of methylene blue and safranin dyes using chitosan zinc oxide nano-beads with *Musa paradisiaca* L. pseudo stem., *Biores. Tech. Rep.*, **5**, 339 (2019).
36. A. B. Rakhym, G. A. Seilkhanova, T. S. Kurmanbayeva: Adsorption of lead (II) ions from water solutions with natural zeolite and chamotte clay, *Mater. Today.*, **31**, 482 (2020).